

# Reaction Modes of Carbonyl Oxide, Dioxirane, and Methylenebis(oxy) with Ethylene: A New Reaction Mechanism

Ramon Crehuet,<sup>†</sup> Josep M. Anglada,<sup>\*,†</sup> Dieter Cremer,<sup>\*,‡</sup> and Josep M. Bofill<sup>§</sup>

Departament de Química Orgànica Biològica, Institut d'Investigacions Químiques i Ambientals de Barcelona, CSIC, C/ Jordi Girona 18, E-08034 Barcelona, Catalunya, Spain, Department of Theoretical Chemistry, University of Göteborg, Reutersgatan 2, S-41320, Göteborg, Sweden, and Departament de Química Orgànica and Centre de Recerca en Química Teòrica, Universitat de Barcelona, Martí i Franquès 1, E-08028-Barcelona, Catalunya, Spain

Received: November 14, 2001; In Final Form: February 1, 2002

The reaction modes of the three isomers, carbonyl oxide (**A**), dioxirane (**B**), and methylenebis(oxy) (**C**), with ethylene (**E**) were investigated by using CASPT2, CCSD(T), and B3LYP with a 6-311+G(2d,2p) basis set. Contrary to general expectations, **A** prefers to react with **E** via a [4+2] cycloaddition reaction (activation enthalpy  $\Delta H^\ddagger(298) = 1.0$  kcal/mol) to yield 1,2-dioxolane (**MA2**) (reaction enthalpy,  $-65.0$  kcal/mol) rather than via an epoxidation reaction ( $\Delta H^\ddagger(298) = 11.3$  kcal/mol) leading to oxirane and formaldehyde. Epoxidation by **B** is slower in view of an activation enthalpy of 13.7 kcal/mol; however, it should proceed stereochemically similar as in the case of **A**. Biradicals **C** and **E** can undergo a pseudo-[4+2] cycloaddition reaction ( $\Delta H^\ddagger(298) = 1.8$  kcal/mol), which leads to 1,3-dioxolane (**MC2**) in a strongly exothermic reaction ( $\Delta H_R(298) = -84.5$  kcal/mol). The results obtained lead to a mechanistic reconsideration of epoxidation reactions observed in the course of the ozonolysis. They also provide a general basis for comparing reactions of 1,3-dipolar compounds and 1,3-biradicals with unsaturated compounds.

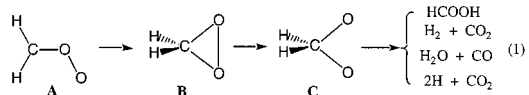
## I. Introduction

Carbonyl oxide (**A**), its cyclic isomer dioxirane (**B**), the corresponding biradical methylenebis(oxy) (**C**), and substituted forms of the three isomers **A**, **B**, and **C** [**AA**, **BB**, **CC**, (please note that dimethyldioxirane or DMDO is a possible isomer of **BB**)] play an important role in several areas of chemistry ranging from synthetic and mechanistic organic chemistry<sup>1–7</sup> to the chemistry of the polluted atmosphere<sup>8–10</sup> as is documented in a large number of reviews. O-oxides **AA** were first discussed in connection with the ozonolysis of unsaturated hydrocarbons<sup>1–7</sup> where they are formed as cycloreversion products of primary ozonides (1,2,3-trioxolanes) according to the Criegee mechanism of the ozonolysis.<sup>11</sup> There is ample evidence on **AA** from trapping experiments<sup>1</sup>; however, the direct spectroscopic identification of **A** or **AA** in general in the ozonolysis reaction was unsuccessful so far.<sup>1–7</sup> Only **B** could be detected in the gas-phase ozonolysis of ethylene (**E**) by microwave spectroscopy.<sup>12</sup> Cremer and co-workers<sup>13</sup> provided theoretical evidence suggesting that a detection of **A** is hardly possible during the ozonolysis because of its kinetic and thermodynamic instability and the fact that **A** is formed with a large amount of excess energy.

Therefore, the most important source of information on **AA** has been the spectroscopic investigation of the oxidation products of diazo compounds utilizing either matrix isolation techniques<sup>5,14,15</sup> or laser flash photolysis in solution with nanosecond time resolution.<sup>5,14</sup> Under these conditions, O-oxides

**AA** are formed as the addition product of singlet or triplet O<sub>2</sub> and the intermediate carbenes generated in the photochemical (thermochemical) decomposition of the diazo compounds. Recently, Sander and co-workers<sup>16</sup> succeeded in synthesizing for the first time a derivative of **A** (dimesityl ketone O-oxide), which is stable at  $-50$  °C in solution and can be investigated by NMR spectroscopy so that detailed information on its structure, stability, and magnetic properties became available.<sup>16,17</sup> The oxidation of diazo compounds also leads to a convenient way of investigating derivatives of **B**,<sup>5,18</sup> although the direct formation of dialkyl substituted **AA** from ketones oxidized by monoperoxyulfuric acid pioneered by Murray<sup>6</sup> is more attractive for the synthetic use of dialkyl **BB**.

There is experimental evidence that reactions of **AA** involve the rearrangement to **BB** and **CC** (reaction 1),<sup>19–22</sup> which is confirmed by theoretical investigations.<sup>23–28</sup>



Calculations reveal<sup>27,28</sup> that once **C** is formed it will rapidly rearrange to acid (or ester in the case of substituted **C**). In the gas phase, there is also the possibility of a decomposition into  $H_2 + CO_2$ ,  $H_2O + CO$ , or  $2H + CO_2$ , either directly or via  $HCOOH$ .<sup>27,28a</sup> Hence, **C** and its derivatives are kinetically and thermodynamically highly unstable, which explains that the biradical has never been observed spectroscopically.<sup>15–17</sup> There is only the indirect evidence for **CC** provided by ester formation from **BB**.<sup>2,5–7</sup>

More than 20 years of intensive theoretical work on isomers **A** and **B** has led to detailed insights on their structure, stability, and reactivity.<sup>13,15–18,23–33</sup> Hence, derivatives of **B** are often used

\* To whom correspondence should be addressed. E-mail: anglada@iiqab.csic.es. E-mail: rcsqt@iiqab.csic.es. E-mail: cremer@theoc.gu.se. E-mail: jmbofill@qo.ub.es.

<sup>†</sup> Institut d'Investigacions Químiques i Ambientals de Barcelona.

<sup>‡</sup> University of Göteborg.

<sup>§</sup> Universitat de Barcelona.

as suitable O transfer agents in stereo- and regioselective epoxidation reactions.<sup>6</sup> Also, **A** is considered to present a strong and therefore less stereoselective epoxidation agent,<sup>1</sup> whereas the role of **C** in epoxidation reactions is not known.

Molecule **A** is considered to be a 1,3-dipolar compound with considerable biradical character.<sup>34</sup> Hence, the preferred reaction mode of **AA** with unsaturated hydrocarbons should be the [4+2] cycloaddition rather than the epoxidation reaction. In the case of **A** reacting with **E**, 1,2-dioxolane (1,2-dioxacyclopentane) should be formed in a symmetry-allowed reaction. In fact, the formation of 1,2-dioxolanes in the ozonolysis of enol ethers was reported by Kuczkowski.<sup>35</sup> Furthermore, Reiser and co-workers<sup>38</sup> and Graziano and co-workers<sup>39</sup> report also formation of 1,2-dioxolanes as a result of cycloaddition reactions between carbonyl oxides **AA** and alkenes. Nevertheless, mechanistic and theoretical work almost exclusively concentrated on the epoxidation reaction of **A**.<sup>29–33</sup> Only the early work by Cremer and Bock<sup>29</sup> considered a cycloaddition between **A** and **E** explicitly where the methods used by these authors did not allow a reliable conclusion as to the magnitude of the energy barriers of cycloaddition and epoxidation reaction. Addition reactions between **B** or **C** and **E** can also not be excluded but would yield 1,3-dioxolane, which was experimentally not observed in reactions involving isomers **B** or **C**.

In view of the fact that the various reaction modes of isomers **A**, **B**, and **C** were never systematically investigated and compared, we present in this work a high level *ab initio* investigation of reactions involving **A**, **B**, **C**, and **E**. The objectives of this work are 3-fold.

(1) We will investigate possible addition reactions between **A**, **B**, **C**, and **E** and compare these reactions with the corresponding epoxidation reactions. This investigation will involve an electronic characterization of the reaction partners with the help of frontier molecular orbital (FMO) theory, the description of transition states (TSs) and intermediates, as well as a reliable calculation of activation and reaction enthalpies.

(2) A special goal of this investigation is to determine reliable thermochemical data (heats of formation) for TSs and labile intermediates, which are difficult to obtain experimentally. Therefore, we will use high level *ab initio* methods with large basis sets to calculate accurate energy differences. However, calculations will also be carried out with density functional theory (DFT) to test whether this theory can be used for chemical problems involving molecules with considerable biradical character.

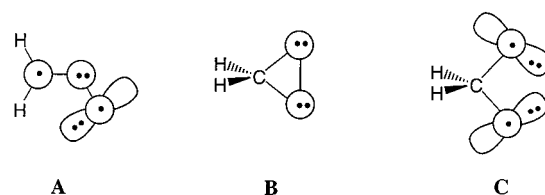
(3) Our investigations will apply to the situation in the gas phase, and therefore, we will discuss results on the background of what role **A**, **B**, **C**, and their derivatives play for the chemistry of the polluted atmosphere. Particular concern will be given to the question whether new experiments can be suggested on the basis of the quantum chemical results.

The results of this investigation are presented as followed. In section 2, we will use FMO theory to characterize the electronic structure changes encountered in reactions of the isomers **A**, **B**, and **C**. In section 3, a description of the computational procedures used in this work is presented. Results of the *ab initio* calculations are discussed in section 4, which is divided into five sections according to the reactions considered in this work. Finally, in section 5, the chemical relevance of the quantum chemical results is discussed and new experimental investigations are suggested.

## II. Electronic Structure Considerations

In Scheme 1, the electronic structures of **A**, **B**, and **C** are given in a simplified way,<sup>40</sup> which indicates partial (**A**) or strong

## SCHEME 1



(**C**) biradical character for two of the three isomers. The corresponding electronic descriptions are indicated in ref 41.

One can distinguish two different reaction modes of **A**, **B**, or **C** with **E**, namely, (a) the concerted O transfer reaction as described in reactions 2 and 3 of Scheme 2 and (b) the concerted addition reactions 4 and 6 of Scheme 3. These two reaction modes correspond to the planar and spiro orientation of the oxidant, respectively, in the reaction with ethylene.

The frontier MOs involved in the O-transfer process from **A** (**B**) to **E** are a lone pair at the terminal oxygen in **A** (the  $\pi$  MOs of the peroxide bridge in **B**), which overlap(s) with the  $\pi^*$  orbital of ethylene (stabilizing interaction 1 in Scheme 2), and the  $\pi$  orbital of **E** which overlaps with the  $\sigma^*(\text{OO})$  orbital of **A** or **B** (stabilizing interaction 2 in Scheme 2). Interaction 1 leads to a cleavage of the  $\pi$ -bond of **E**, whereas interaction 2 triggers the OO bond rupture. The charge transfer from the  $\pi$  MO of **E** into the  $\sigma^*(\text{OO})$  orbital is complemented by back-donation from the lone pair lp(O) orbital thus yielding the two  $\sigma(\text{CO})$  orbitals of the oxirane ring as originally described by Dewar<sup>42</sup> and extensively studied by Cremer and Kraka.<sup>43</sup>

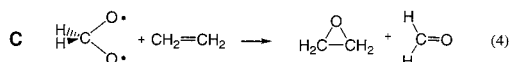
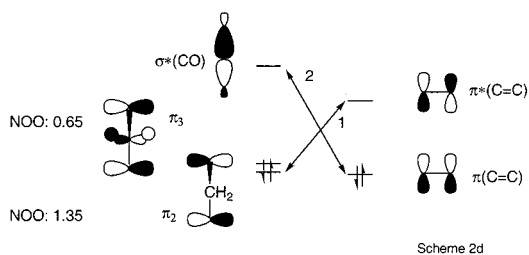
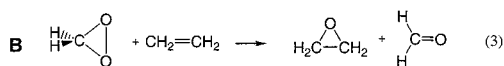
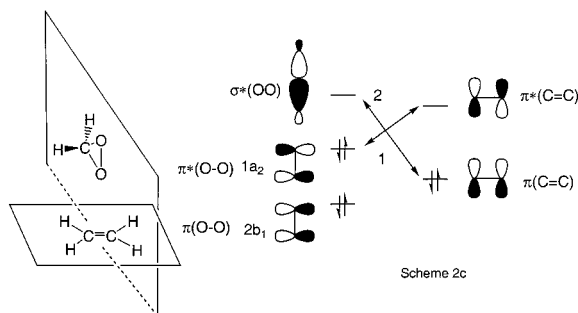
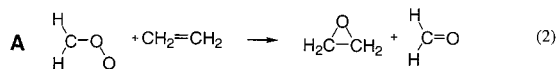
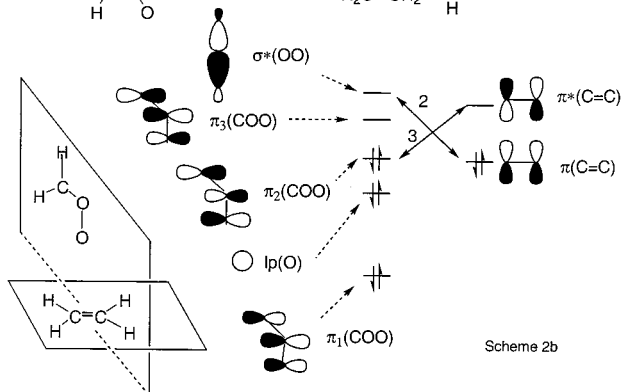
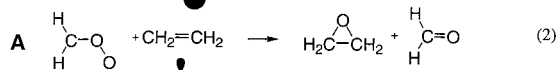
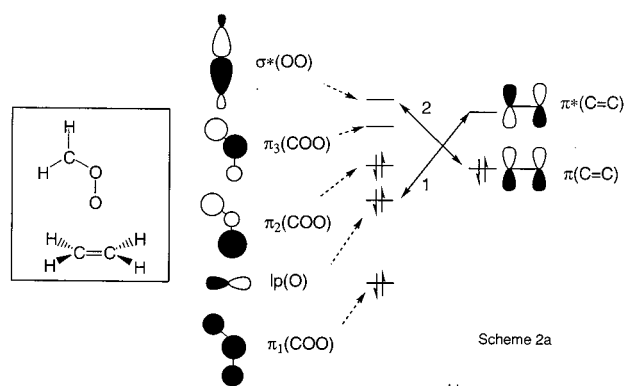
Analysis of the interaction diagrams in Scheme 2 leads to a number of predictions with regard to the stereochemistry of the O transfer and the reactivity of isomers **A**, **B**, and **C** in epoxidations reactions:

(a) The best approach for **A** to **E** is in the way given in Scheme 2a (see also Figure 1a); that is, all heavy atoms are in one plane because this leads to the strongest interactions 1 and 2. If, however, the COO plane of **A** is perpendicular to the CC bond, interaction 3 rather than 1 has to be considered (see Scheme 2b). Again, this interaction implies a weakening of the  $\pi$ -bond of **E**; however, at the same time, it also leads to a strengthening of the OO bond of **A** because MO  $\pi_2$  is OO antibonding and its depopulation decreases the OO-antibonding nature. We find in agreement with this prediction that the true TS of reaction 2 has all heavy atoms in one plane, whereas a rotation of **A** by 90° leads to a second-order TS (see also ref 31). In the case of **B**, (reaction 3, Scheme 2c), interactions 1 and 2 will be largest if the COO ring is perpendicular to the double bond of **E**. Rotation by 90° leads to repulsion between the two molecules and increases the energy.

(b) On the basis of interaction diagrams such as those given in Scheme 2 (Figure 1 parts a and b), it is difficult to predict the magnitude of the reaction barrier for O transfer. However, it is clear that in the case of **B** the cleavage of the OO bond as the weaker bond (both  $\pi(\text{OO})$  and  $\pi^*(\text{OO})$  are doubly occupied) will initialize the O transfer, which also implies the cleavage of one of the CO bonds and the formation of a new  $\pi(\text{CO})$  MO from previous  $\sigma$  MOs (OO and CO). The OO bond in **A** is somewhat stronger and, therefore, the corresponding barrier for O transfer should be somewhat higher as in the case of **B**.

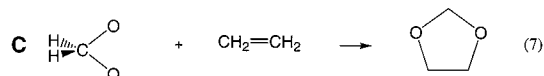
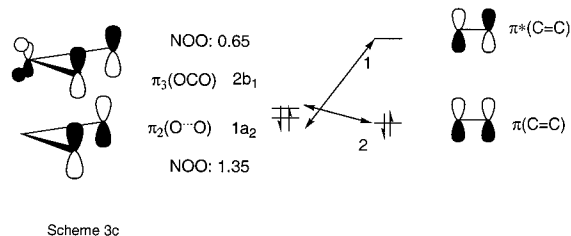
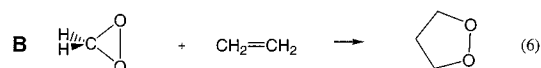
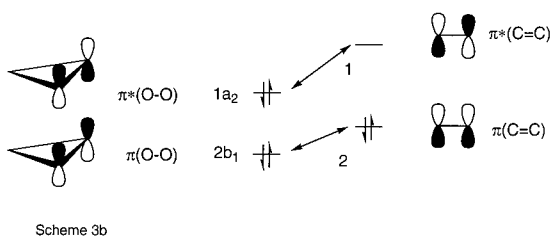
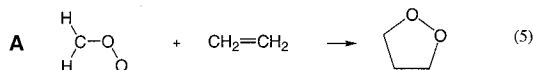
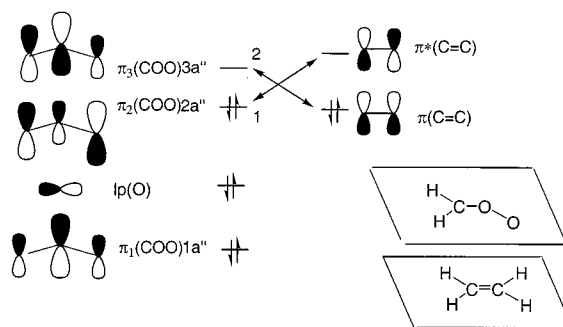
(c) In the case of the epoxidation of **E** and smaller alkenes, there should be no difference with regard to the stereochemistry of the reaction; that is, both **A** and **B** should stereospecifically epoxidize *cis* (trans) alkene to *cis* (trans) oxirane. However, for alkenes with bulky substituents, the central approach of the

## SCHEME 2



terminal O atom of **A** to the double bond will become more difficult, and instead, the C atom with less bulky groups will

## SCHEME 3



be attacked. In the extreme, this may lead to a change in the TS geometry or a loss of the stereospecificity of epoxidation.

(d) For **C** (reaction 4, Scheme 2d), a CO bond has to be broken to initiate an O transfer. However, the  $\sigma^*(\text{CO})$  MO is higher in energy than the  $\sigma^*(\text{OO})$  MO, and therefore, interaction 2 is much weaker as in the case of **A** or **B**. In addition, back-donation from the terminal O atom to the  $\pi^*$  MO of **E** will not lead to a change in CO bonding if  $\pi_2$  ( $1a_2$ ) MO is involved. However, it will lead to a strengthening of the CO bond if the  $\pi_3$  ( $2b_1$ ) MO is involved (Scheme 2d). According to CASSCF-(18,14) calculations, the natural orbital occupation (NOO) numbers are 1.35 and 0.65 for these MOs thus reflecting the biradical character of **C**. This is also reflected looking at the  $S^2$  expectation value of the UCCSD(T) wave function, which is 1.007 and 0.13 before and after spin projection, respectively. Under normal conditions, **C** should not react as an epoxidation agent. One can express this by saying that O transfer requires a peroxide unit with a  $4\pi$  system, which is not given in the case of **C**.

The addition reactions between **A**, **B**, or **C** and **E** (reactions 5, 6, and 7 in Scheme 3, Figure 1 parts c and d) can be

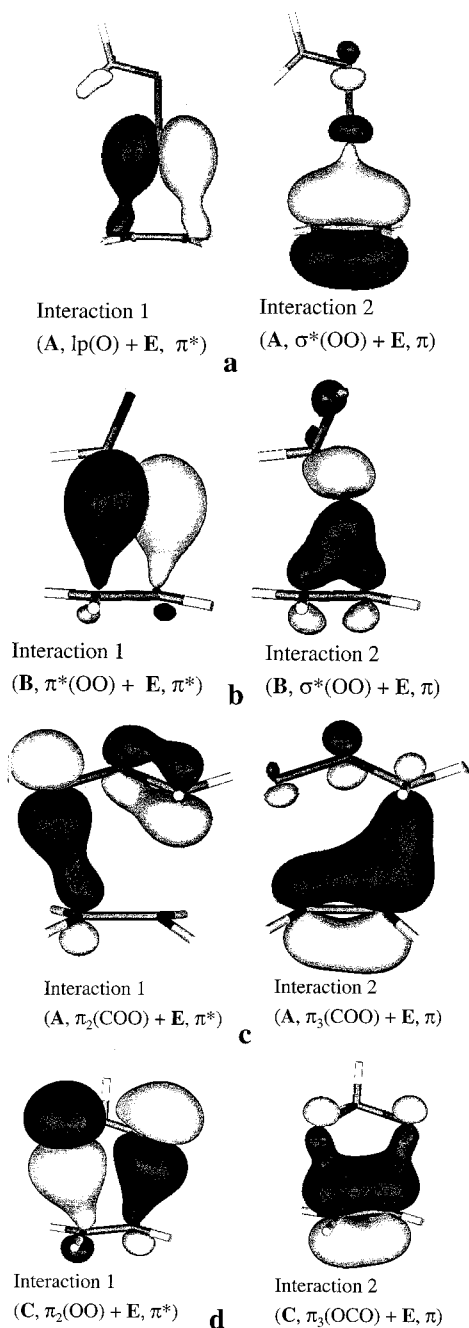


**Figure 1.** HOMO and sub-HOMO of the transition state of four different reactions between **A**, **B**, **C**, and **E**. (a) Epoxidation of ethylene by carbonyl oxide. (b) Epoxidation of ethylene by dioxirane. (c) Cycloaddition between ethylene and carbonyl oxide. (d) Cycloaddition between ethylene and methylenebis(oxy). The notation of the MOs is given. On the left side, the MOs corresponding to interactions 1 and, on the right side, the MOs corresponding to interactions 2 in Schemes 2 and 3 are shown.

considered as reactions involving just the frontier  $\pi$  MOs of the reaction partners. Interactions 1 (between  $\pi_2$  of **A** and  $\pi^*$  of **E**) and 2 (between  $\pi$  of **E** and  $\pi_3$  of **A**, Scheme 3a, Figure 1c) lead to a new CC and a new CO bond including the destruction (preservation) of the  $\pi$  bonds ( $\sigma$  bonds) in **A** and **E** thus yielding 1,2-dioxolane (reaction 5). There is also a weakly repulsive interaction between  $\pi_1(\mathbf{A})$  and  $\pi(\mathbf{E})$ ; however, this does not hinder a reactive collision between **A** and **E**.

In the case of **B**, interaction 2 is destabilizing thus hindering the formation of 1,3-dioxolane (reaction 6, Scheme 3b). However, if a collision between **B** and **E** leads to **C**, an addition

to **E** and the formation of 1,3-dioxolane will become possible (reaction 7, Scheme 3c). In view of the fact that **C** possesses three  $\pi$ -type MOs ( $1b_1$ , pseudo- $\pi$  ( $\text{CH}_2$ ) with small bonding  $\pi(\text{CO})$  character;  $1a_2$ , nonbonding  $\pi(\text{CO})$  and through-space  $\pi(\text{OO})$  antibonding character; and  $2b_1$ , small antibonding  $\pi(\text{CO})$  and through-space  $\pi(\text{OO})$  bonding character), two of which are occupied, we consider **C** as a pseudo- $4\pi$  system, which can undergo a symmetry-allowed pseudo-[4+2] cycloaddition reaction with **E**. As in the case of **A**, bonding to **E** is established by interactions 1 and 2 (Figure 1d). There is a large similarity in the interactions diagrams for **A** and **C** (Scheme 3), and therefore, we consider the corresponding reactions as symmetry-allowed concerted pericyclic  $\pi$ - $\pi$  reactions leading to a destruction of the  $\pi$  systems of the reaction partners. Because for the O-transfer reactions both  $\sigma$  and  $\pi$  bonds are changed, we will use the term  $\sigma$ - $\pi$  reactions for reactions 2 and 3.

As an important result of this analysis we find that, despite their different structures, molecules such as ozone **A** or **C** (in general 1,3-dipolar molecules and 1,3-biradicals) should show a similar reactivity with regard to unsaturated compounds (alkenes, alkynes, ketones, etc.) in the way that they all can lead either to five-membered rings or epoxidation products (X- or Z-transfer products if a general system XYZ is considered). The similarity of the reactive behavior in  $\pi$ - $\pi$  reactions is caused by the biradical character found for 1,3-dipolar molecules and molecules such as **C**.<sup>34,44</sup> For example, the ground electronic state of  $\text{O}_3$  possesses considerable biradical character<sup>34,44,45</sup> as does that of **A**. Hence, it is reasonable to predict that all of these species undergo cycloaddition reactions with unsaturated molecules in a similar way, i.e., with comparably low activation energies. **B** does not contain any biradical character and, accordingly, does not react in the  $\pi$ - $\pi$  fashion. Epoxidation (X/Z transfer) will occur if a  $\sigma^*(\text{OO})$  MO ( $\sigma^*(\text{XY})$  or  $\sigma^*(\text{YZ})$  MO) can be occupied, which is low in energy.

### III. Computational Details

The molecular geometries of the stationary points on the potential energy surfaces (PESs) were optimized using the CASSCF method<sup>46</sup> employing analytical gradient procedures.<sup>47-49</sup> The complete active space of a given structure was selected according to the fractional occupation of the natural orbitals (NOs)<sup>50</sup> generated from the first-order density matrix of a MRD-CI<sup>51-53</sup> wave function based on the correlation of all valence electrons. The active space composition changes for the different reactions studied, and the corresponding dimensions range among 1764 and 19404 symmetry adapted functions. The details of the different active spaces used are collected in Table 1 of the Supporting Information.

In a preliminary step, CASSCF geometry optimizations and the characterization of the stationary points as minima or saddle points were carried out using the split-valence-d-polarized 6-31G(d) basis set.<sup>54</sup> The topology of the PES, i.e., the connectivity between a given TS and the reactant/product minima, was verified in each case by performing intrinsic reaction coordinate (IRC) calculations<sup>55</sup> at the same level of theory. The zero-point vibrational energies (ZPVE) determined from the CASSCF/6-31G(d) harmonic vibrational frequencies were scaled by 0.8929<sup>56</sup> and were used to calculate the thermochemical corrections for obtaining enthalpies at 298 K. In a second step, all CASSCF geometries were reoptimized using the more flexible 6-311+G(2d,2p) basis set.<sup>57</sup>

In a third step, the effects of dynamic valence-electron correlation on CASSCF energy differences were covered in two different ways. First, we performed CASPT2<sup>58</sup> single-point



calculations based on a common CASSCF(10,10) reference function. The latter was chosen because the (10,10) active space corresponds to the sum of the appropriate active spaces describing the reactants **A** or **C** plus ethylene for  $\sigma-\pi$  or  $\pi-\pi$  reactions.<sup>25,28</sup> Second, single-point energy calculations were performed using the CCSD(T) method.<sup>59,60</sup> For those structures showing a clear biradical (or multireference) character, the CCSD(T) calculations were based on a reference UHF wave function of broken symmetry. The T1 diagnostic of Lee<sup>61</sup> and the expectation value of  $S^2$  were computed to check the reliability of the UHF-CCSD(T) results where in the case of the  $\langle S^2 \rangle$  value the energy-relevant part was analyzed according to He and Cremer.<sup>62</sup> All single-point calculations were performed with the 6-311+G(2d,2p) basis set utilizing CASSCF/6-311+G(2d,2p) geometries.

In the case of van der Waals complexes, the basis set superposition error (BSSE) was corrected with the help of the counterpoise method of Boys and Bernardi.<sup>63</sup> These calculations were done at the CCSD(T) level of theory.

In a fourth step, we reoptimized and characterized all stationary points employing DFT with the hybrid functional B3LYP<sup>64</sup> and the 6-31G(d,p) basis set. B3LYP/6-31G(d,p) vibrational frequencies were scaled by 0.9806 as suggested by Scott and Radom.<sup>65</sup> Finally, all B3LYP geometries were reoptimized using the 6-311+G(2d,2p) basis set. The objectives of these calculations were 2-fold: DFT covers a considerable amount of correlation effects,<sup>66</sup> and therefore, it was possible to test the influence of a larger basis set on geometries at a correlation corrected level. Second, it is interesting to compare UB3LYP, CASSCF/CASPT2, and UHF-CCSD(T) results for biradicals. For  $\sigma,\sigma$  and  $\pi,\pi$  biradicals, UDFT has been found to lead to surprisingly accurate descriptions, whereas for  $\sigma,\pi$ -biradicals it fails for principal reasons.<sup>67-69</sup> If these observations can be confirmed in the present case, then there will be a chance of investigating at B3LYP substituted derivatives of **A**, **B**, and **C**, which are directly relevant for synthetic work or atmospheric studies.

For all of the stationary points, thermochemical corrections and entropies  $S$  were determined to obtain absolute enthalpies  $H$  and Gibbs free energies  $G$  at 298 K and, accordingly, enthalpy differences  $\Delta H(298)$  and  $\Delta G(298)$ . Reaction enthalpies are denoted as  $\Delta H_R(298)$  and activation enthalpies as  $\Delta H^\ddagger(298)$ . Utilizing experimental heats of formation  $\Delta H_f^\circ(298)$ <sup>70</sup> heats of formation  $\Delta H_f^\circ(298)$  were derived for all stationary points to facilitate the analysis of quantum chemical results and to increase their compatibility to measured thermochemical data. For each reaction step, the most reliable enthalpy difference was selected according to criteria explicitly discussed in the Supporting Information. In a number of cases,  $\Delta H_f^\circ(298)$  values were also derived from group increments using Benson's approach.<sup>71</sup>

The quantum chemical calculations were carried out by using the GAMESS,<sup>72</sup> the Gaussian 94,<sup>73</sup> and the Molcas 4.1<sup>74</sup> program packages.

#### IV. Results and Discussion

Relative energies, enthalpies, Gibbs free energies, ZPVE, entropies, dipole moments, and heats of formation calculated in this work are summarized in Tables 1 and 2. Relevant geometrical parameters of all stationary points are displayed in Figures 2, 3, and 5. Figures 4 and 6 give schematically the most reliable set of enthalpy differences and heats of formations for the reactions between **A**, **C**, and **E**. The full set of results (Cartesian coordinates of all stationary points and all CASSCF,

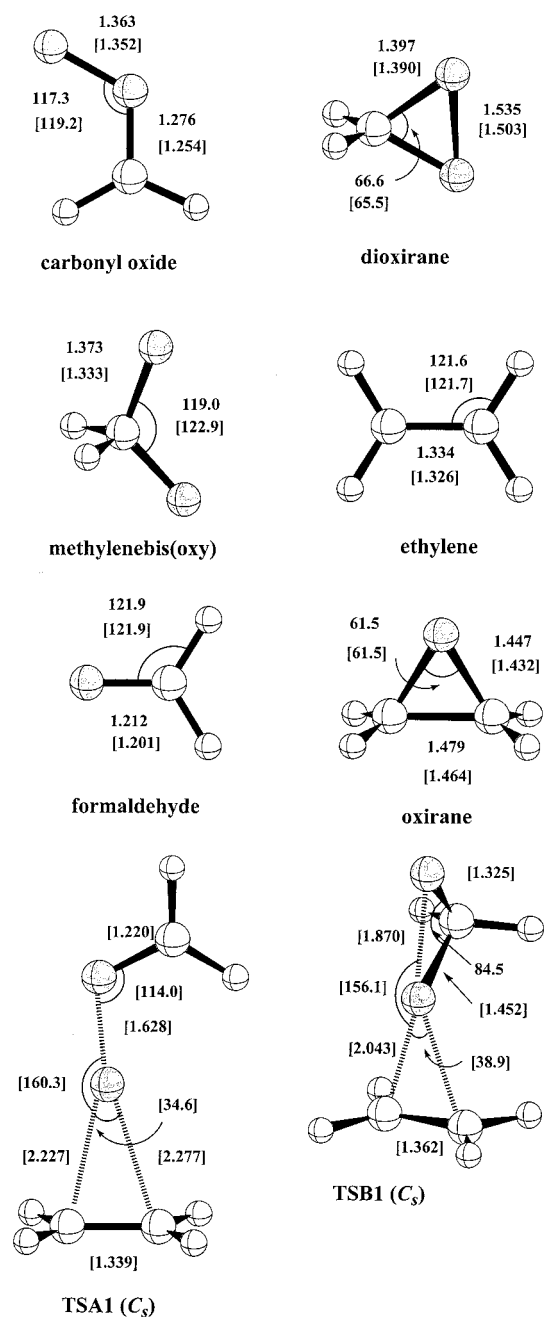


**Figure 2.** Selected geometrical parameters of the CASSCF/6-311+G(2d,2p) (and B3LYP/6-311+G(2d,2p) in brackets) optimized structures of the reactants, products, and the transition states involved in the ethylene epoxidation.

CCSD(T), CASPT2, and B3LYP absolute energies of all structures) is given in the Supporting Information.

Throughout the text, the structures of the stationary points are designated by **M** for minima and by **TS** for transition states followed by the letters **A**, **B**, or **C** depending on which isomer reacts with **E**. Each structure acronym is appended by the numbers 1, 2, 3, etc. according to its occurrence along the reaction path. Thus, **TSA1** refers to transition state 1 of the reaction between **A** and **E**, whereas **TSC1** corresponds to transition state 1 of the reaction between **C** and **E**.

In the following discussion, we discuss exclusively the heats of formation listed in the last column of Tables 1 and 2 rather than discussing the reliability and errors of the various methods/basis set combinations used (see the Supporting Information).

**TABLE 1: Relative Energies, Zero-Point Energies, Entropies, Free Energies, and Dipole Moments for the Reactions of A and B with E Computed with Different Methods Using the 6-311+G(2d,2p) Basis Set<sup>a</sup>**

compound	relative to	method	DE	ZPE	S	DH(298)	DG(298)	<i>m</i>	$\Delta H_f^\circ(298)^b$
<b>A + C<sub>2</sub>H<sub>4</sub></b>	<b>A + C<sub>2</sub>H<sub>4</sub></b>	CASPT2	0	47.9	114.7	0	0	4.33	<b>39.5*</b>
		CCSD(T)	0			0	0		
<b>TSA1</b>	<b>A + C<sub>2</sub>H<sub>4</sub></b>	RB3LYP	0	50.7	111.9	0	0	4.39	<b>50.8</b>
		CCSD(T)	11.3			11.3	20.3		
<b>MA1</b>	<b>A + C<sub>2</sub>H<sub>4</sub></b>	RB3LYP	11.1	50.8	81.7	11.1	20.1	3.91	<b>38.8</b>
		CASPT2	-2.3	48.4	93.6	-1.0	5.1	4.25	
<b>TSA2</b>	<b>MA1</b>	CCSD(T)	-2.5			-1.2	4.9		<b>39.8</b>
		CCSD(T)+BSSE	-2.0			-0.7	4.5		
		RB3LYP	-1.7	51.7	87.9	-0.3	6.9	4.29	
		CASPT2	-1.2	50.6	72.3	-1.7	2.2	3.05	
<b>MA2</b>	<b>TSA2</b>	CCSD(T)	1.5			1.0	4.9		<b>7.4</b>
		RB3LYP	2.5	52.5	74.8	2.0	5.9	3.58	
<b>TSA3</b>	<b>MA2</b>	CASPT2	-60.2	54.4	69.3	-56.4	-55.5	3.18	<b>8.1</b>
		CCSD(T)	-63.0			-59.2	-58.36		
<b>MA3</b>	<b>TSA3</b>	RB3LYP	-59.7	56.6	69.7	-56.3	-54.7	3.12	<b>4.7</b>
		CASPT2	30.7	53.2	69.1	29.4	29.5	3.29	
<b>TSA4</b>	<b>MA3</b>	CCSD(T)	34.8			33.6	33.6		<b>13.8</b>
		UB3LYP	29.8	52.6	72.2	26.0	25.2	3.67	
<b>MA4</b>	<b>TSA4</b>	CASPT2	-1.1	52.8	74.1	-1.1	-2.6	2.10	<b>15.6</b>
		CCSD(T)	-3.5			-3.4	-5.0		
<b>TSA5</b>	<b>MA4</b>	UB3LYP	-3.9	52.7	73.2	-3.4	-3.7	2.2	<b>18.8</b>
		CASPT2	3.7	52.4	71.3	2.8	3.6	1.32	
<b>TSA6</b>	<b>MA2</b>	CCSD(T)	3.6			2.7	3.5		<b>13.2</b>
		UB3LYP	3.1	52.0	72.6	2.1	2.3	1.58	
<b>MA5</b>	<b>TSA7</b>	CASPT2	-2.6	52.5	74.4	-2.0	-2.9	2.12	<b>15.6</b>
		CCSD(T)	-2.4			-1.8	-2.7		
<b>TSA7</b>	<b>MA3</b>	UB3LYP	-2.2	52.4	75.4	-1.4	-2.2	2.48	<b>13.8</b>
		CASPT2	2.7	51.0	75.5	1.2	0.8	2.02	
<b>MA5 + H<sub>2</sub>CO</b>	<b>TSA7</b>	B3LYP	8.4	52.1	75.9	8.2	8.0	2.26	<b>15.6</b>
		CASPT2	44.9	50.3	76.3	41.1	39.0	4.35	
<b>TSA8 + H<sub>2</sub>CO</b>	<b>MA5 + H<sub>2</sub>CO</b>	UB3LYP	41.4	50.0	77.7	35.8	33.4	5.18	<b>13.2</b>
		CASPT2	16.9	50.1	75.3	14.1	13.8	2.67	
<b>H<sub>2</sub>CO+oxirane</b>	<b>TSA8 + H<sub>2</sub>CO</b>	UB3LYP	14.9	49.7	78.7	12.4	10.7	3.01	<b>14.1</b>
		CASPT2	-2.8	46.4	116.7	-5.6	-17.9	2.16	
<b>TSA9</b>	<b>B + C<sub>2</sub>H<sub>4</sub></b>	UB3LYP	-4.5	47.0	117.8	-6.2	-17.8	3.19	<b>61.1</b>
		CASPT2	1.1	46.5	114.8	0.9	1.4	2.06	
		CCSD(T)	1.0			0.7	1.3		
		UB3LYP	2.9	53.8	115.1	3.1	3.9	2.73	
<b>B + C<sub>2</sub>H<sub>4</sub></b>	<b>A + C<sub>2</sub>H<sub>4</sub></b>	CASPT2	-55.7	52.0	117.5	-52.3	-51.3		<b>12.2*</b>
		CCSD(T)	-59.1			-55.6	-54.6		
<b>TSB1</b>	<b>B + C<sub>2</sub>H<sub>4</sub></b>	RB3LYP	-53.8	51.9	111.6	-49.8	-48.8		<b>13.4*</b>
		CASPT2	21.5	48.6	77.2	21.6	32.8	1.69	
<b>C + C<sub>2</sub>H<sub>4</sub></b>	<b>B + C<sub>2</sub>H<sub>4</sub></b>	CASPT2	-24.3	49.3	112.6	-23.1	-22.5		<b>25.9</b>
		CCSD(T)	-24.2			-23.1	-22.4		
<b>C + C<sub>2</sub>H<sub>4</sub></b>	<b>B + C<sub>2</sub>H<sub>4</sub></b>	RB3LYP	-20.7	51.5	109.8	-20.0	-19.4		<b>13.0; 13.4*</b>
		CCSD(T)	13.7			13.7	23.5		
<b>C + C<sub>2</sub>H<sub>4</sub></b>	<b>B + C<sub>2</sub>H<sub>4</sub></b>	RB3LYP	13.1	52.3	77.7	13.2	22.9	4.99	
		CASPT2	6.9	47.4	113.6	5.2	4.9	2.16	
<b>C + C<sub>2</sub>H<sub>4</sub></b>	<b>B + C<sub>2</sub>H<sub>4</sub></b>	CCSD(T)	11.6			9.8	9.5		
		UB3LYP	3.8	48.3	111.4	0.8	0.3	2.50	

<sup>a</sup> Relative energies, ZPE values, relative enthalpies, and relative free energies in kcal/mol, entropies *S* in cal mol/deg, and dipole moments *m* in Debye. ZPE, *S*, and thermodynamic corrections were calculated at the CASSCF/6-31G(d) and B3LYP/6-31G(d,p) levels of theory. Heats of formations  $\Delta H_f^\circ(298)$  (in kcal/mol) are given for the best calculation (see explanations in the Supporting Information) relative to the known  $\Delta H_f^\circ(298)$  values for **A + E**, **B + E**, and **C + E** (ref 15) indicated by a star and compared where possible with experimental values from ref 70 also indicated by a star. <sup>b</sup> Computed at B3LYP/6-311+G(2d,2p) optimized geometries.

In this way, just the chemical relevant aspects of the investigation rather than technical aspects are considered.

**IV.1. Carbonyl Oxide (A), Dioxirane (B), and Methylenebis(oxy) (C).** The calculated geometries of **A**, **B**, and **C** (Figure 2) compare well with other theoretical results published previously<sup>23–28,30,75–77</sup> and with the experimental structure of **B**.<sup>12,78</sup> The computed relative energies of the three isomers differ from the best results so far obtained by about 4 kcal/mol,<sup>27</sup> which is typical of calculations of peroxides carried out without f-type polarization functions.<sup>76</sup> Hence, the enthalpy difference between **A** and **B** is calculated to be -23.1 kcal/mol, whereas the more reliable value obtained by Cremer et al. is -27.0 kcal/mol.<sup>27</sup> Similarly, the stability of **C** relative to **B** is underestimated

by 4 kcal/mol at the CASPT2 level of theory.<sup>79</sup> Using the MR-AQCC results of ref 27, we corrected the relative enthalpies of **A**, **B**, and **C** and set the heats of formation of **A + E**, **B + E**, and **C + E** to 39.5, 12.2, and 13.4 kcal/mol (see Supporting Information), respectively, utilizing  $\Delta H_f^\circ(E) = 12.54$  kcal/mol.<sup>70</sup>

**IV.2. Ethylene Epoxidation by Carbonyl Oxide and Dioxirane.** The epoxidation of **E** by **A** and/or **B** was extensively investigated in previous theoretical studies.<sup>29–33</sup> The CCSD(T)/6-311+G(2d,2p)//B3LYP/6-311+G(2d,2p) activation enthalpies  $\Delta H^\ddagger(298)$  of 11.3 and 13.7 kcal/mol, respectively, obtained in this work (**TSA1** and **TSB1**; Table 1, Figure 4) agree

**TABLE 2: Relative Energies, Zero-Point Energies, Entropies, Free Energies, and Dipole Moments for the Reaction of Biradical C with Ethylene, Computed with Different Methods Using the 6-311+G(2d,2p) Basis Set<sup>a</sup>**

compound	relative to	method	DE	ZPE	S	DH(298)	DG(298)	m	$\Delta H_f^\circ(298)^b$
<b>C + C<sub>2</sub>H<sub>4</sub></b>	<b>B + C<sub>2</sub>H<sub>4</sub></b>	CASPT2	0	47.4	113.6	0	4.9	2.16	<b>13.4*</b>
		CCSD(T)	0			0	0		
		UB3LYP	0	48.3	111.4	0	0		
<b>MC1</b>	<b>C + C<sub>2</sub>H<sub>4</sub></b>	CASPT2	-1.9	47.7	95.1	-0.8	4.7	2.03	<b>13.0</b>
		CCSD(T)	-1.5			-0.5	5.1		
		CCSD(T)+BSSE	-1.4			-0.4	5.0		
		UB3LYP	-0.8	48.2	95.1	-0.5	4.3	2.34	
<b>TSC1</b>	<b>MCI</b>	CASPT2	-3.0	50.1	75.1	-2.0	4.0	1.39	<b>14.8</b>
		CCSD(T)	-3.1			-2.1	3.9		
		UB3LYP	1.2	50.1	75.9	1.8	7.5	1.47	
<b>MC2</b>	<b>TSCI</b>	CASPT2	-88.9	55.7	70.6	-83.2	-81.9	1.30	-72.6; <b>-71.1*</b>
		CCSD(T)	-93.1			-87.5	-86.2		
		RB3LYP	-88.7	57.2	71.5	-82.1	-80.8	1.24	

<sup>a</sup> Relative energies, ZPE values, relative enthalpies, and relative free energies in kcal/mol, entropies *S* in cal mol/deg, and dipole moments *m* in Debye. ZPE, *S*, and thermodynamic corrections were calculated at the CASSCF/6-31G(d) and B3LYP/6-31G(d,p) levels of theory. Heats of formations  $\Delta H_f^\circ(298)$  (kcal/mol) are given for the best calculation in bold print; they were derived relative to the known  $\Delta H_f^\circ(298)$  values for **C + E** (**C**, 0.9 kcal/mol, ref 27) and are compared where possible with experimental values from ref 70: **E**, 12.54; CH<sub>2</sub>=O, -27.70; CH<sub>3</sub>CH=O, -39.73; oxirane, -12.58; 1,3-dioxolane, -71.1 kcal/mol. A star connected with *est* denotes values obtained from thermochemical group increments.<sup>71</sup> For details concerning the determination of heats of formation, see the Supporting Information. <sup>b</sup> Computed at B3LYP/6-311+G(2d,2p) optimized geometries.

well with other results from the literature. The COO unit of **A** is in a common plane with the CC atoms of **E** as predicted in section II. Rotation of COO by 90° leads to a second-order TS higher in energy by 0.9 kcal/mol. The electronic features of the epoxidation of **E** are similar to other O atom transfer reactions between **A** and double bonds. For instance, we have found a reaction path between H<sub>2</sub>COO and H<sub>2</sub>CO that produces directly **B** plus H<sub>2</sub>CO with an activation energy of 14.2 kcal/mol.<sup>80</sup>

In addition to the concerted epoxidation reaction between **A** and **E**, we found also a stepwise epoxidation mode proceeding via **TSA9** (Figure 3). In this mode, **A** approaches **E** in a parallel plane in an end-on rather than side-on fashion so that a [4+2] cycloaddition is not possible. O is transferred to **E** yielding biradical **MA5** and H<sub>2</sub>CO. Rotation at the CC bond in **MA5** leads to **TSA8** (activation enthalpy, 0.9 kcal/mol; Table 1, Figure 4), and the bonding overlap between the single-electron orbitals yields oxirane. The computed activation enthalpy is 21.6 kcal/mol and by this twice as large as epoxidation via **TSA1**. The reaction will only be possible if **A** is formed in the gas phase with a considerable amount of excess energy as is the case in the ozonolysis reaction (provided the concentration of **E** is high enough). On the other hand, the stepwise epoxidation via **TSA9** may become interesting in the presence of asymmetrically substituted alkenes such as isobutene reacting with highly substituted **A** such as bis(mesityl)carbonyl oxide.<sup>16,17</sup>

**IV.3. Formation of 1,2-Dioxolane.** Reaction 5 in Scheme 3a is a symmetry-allowed [4+2] cycloaddition reaction, which leads to 1,2-dioxolane (**MA2**). This reaction is initiated by the formation of van der Waals complex **MA1**, which after BSSE corrections is 0.7 kcal/mol ( $\Delta H(298)$  value, Table 1;  $\Delta E = -2.0$  kcal/mol) more stable than **A + E** and arranges the latter in a form they have to adopt in **TSA2** of the cycloaddition reaction 5. Figure 3 shows that **MA1** and **TSA2** adopt an envelope-like conformation similar as the **E**-ozone complex<sup>81,82</sup> and 1,2,3-trioxolane (primary ozonide) in the ethylene ozonolysis do.<sup>28,83-85</sup> The most interesting geometrical features of **TSA2** (see Figure 3) are the C••C and C••O interaction distances of 2.20 and 2.27 Å, respectively, which are clearly longer than a normal CC or CO bond formed (broken) in a TS (ca. 2 Å). The CO and OO bond lengths of the carbonyl oxide and ethylene unit have values (1.290, 1.368, and 1.394 Å, Figure 3) similar to those calculated for **A** and **E** (1.276, 1.363, and 1.334 Å, Figure 2). This indicates

that the  $\pi$  bonds of **A** and **E** are largely retained in **TSA2** in line with an early TS of a strongly exothermic reaction.

The CCSD(T) activation enthalpy is 1.0 kcal/mol, which is significantly lower than the corresponding value of 11.3 kcal/mol computed for the epoxidation reaction (Table 1, Figure 4) but which is similar to the calculated activation enthalpies for the [4+2]-cycloaddition of O<sub>3</sub> + **E** or **A** + H<sub>2</sub>CO.<sup>25,28,86</sup> Consequently, [4+2] cycloaddition rather than epoxidation should be the preferred reaction mode between **A** and **E** (see section V).

Cremer<sup>87</sup> described **MA2** as a hindered pseudorotor with a barrier to pseudorotation of just 2.2 kcal/mol and a barrier of inversion through the planar form of 5.7 kcal/mol. The C<sub>2</sub> symmetrical twist form (Figure 3) is the most stable form, whereas the C<sub>s</sub> symmetrical envelope form is located at the TS of pseudorotation. The calculated puckering amplitude *q* = 0.467 Å is somewhat larger than the HF/6-31G(d) value of 0.451 Å<sup>87</sup> and the experimental value of 0.45 Å<sup>87</sup> (B3LYP, 0.442 Å), which simply results from the fact that the CASSCF geometry exaggerates all bond lengths: *R*(OO) = 1.476 (1.461, ref 87) Å, *R*(CO) = 1.444 (1.439) Å, and *R*(CC) = 1.558 (1.543) Å.

Formation of **MA2** is exothermic by 65.0 kcal/mol (Figure 4). We calculate a heat of formation  $\Delta H_f^\circ(298, \mathbf{MA2})$  of -25.5 kcal/mol where this value is based on the experimental  $\Delta H_f^\circ(298)$  value of 1,3-dioxolane (**MC2**, -71.1 kcal/mol<sup>70</sup>) and the calculated enthalpy difference between **MA2** and **MC2** (45.6 kcal/mol at CCSD(T), see the Supporting Information).

**IV.4. Formation of Ethylene Epoxide from 1,2-Dioxolane.** Because **MA2** will be formed with an excess energy of 65 kcal/mol, it can undergo, at least in the gas phase but probably also in solution, a unimolecular decomposition process. In connection with the direct ethylene epoxidation described above, we have found two reaction mechanisms, (a) + (b), which lead to the formation of ethylene epoxide from 1,2-dioxolane and that correspond to (a) a stepwise decomposition leading to biradical intermediates and to (b) a concerted decomposition reaction of the  $\pi, \pi$ -type discussed in section 2. A further investigation on the unimolecular decomposition of 1,2-dioxolane is underway and will be presented elsewhere.<sup>89</sup>

(a) The cleavage of the OO bond in **MA2** leading to biradical OCH<sub>2</sub>CH<sub>2</sub>CH<sub>2</sub>O, for which we have found two isomers, **MA3** and **MA4** interconnected through the transition state **TSA4**. The reaction is endothermic by about 30 kcal/mol, and the calculated

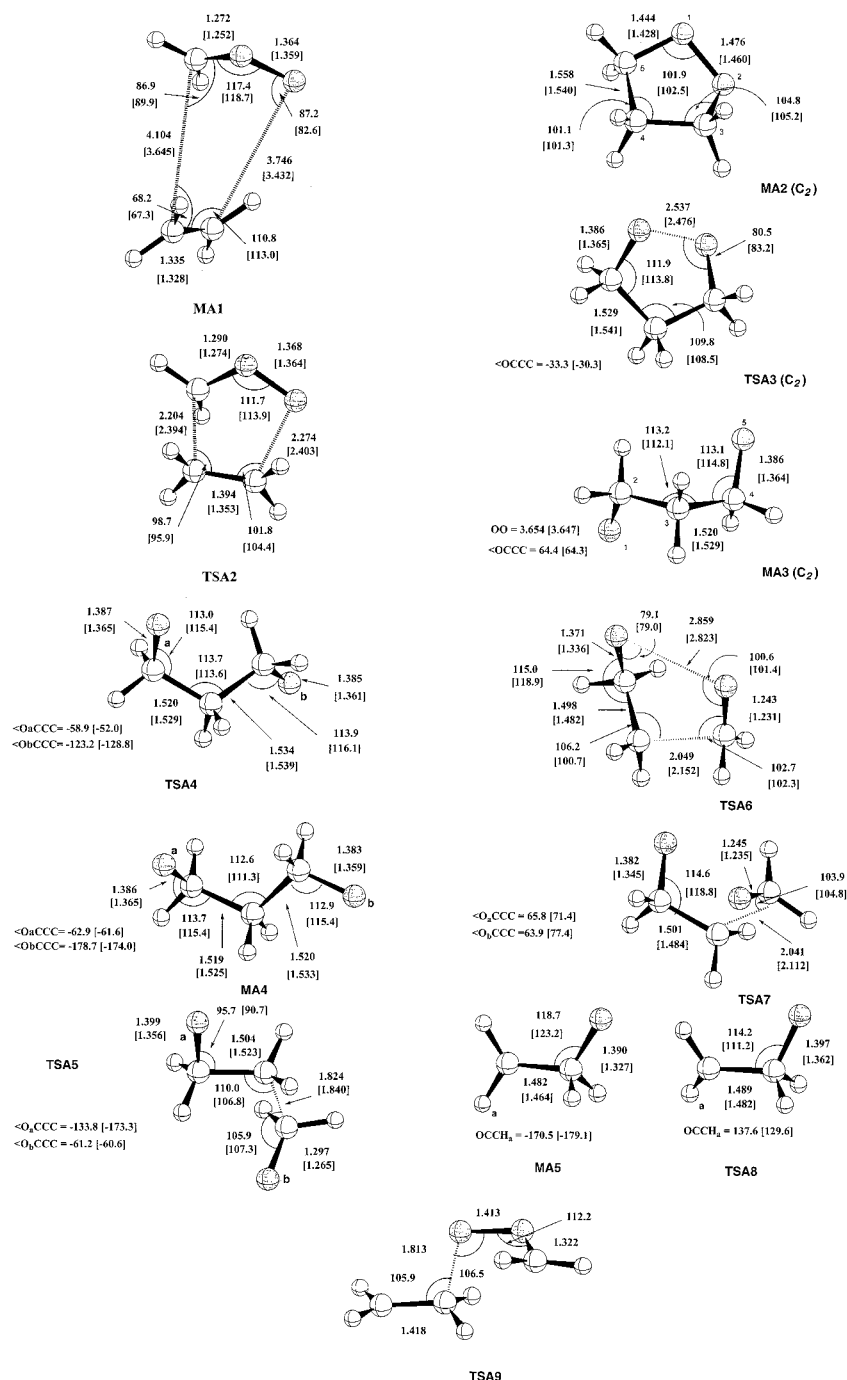


**Figure 3.** Selected geometrical parameters of the CASSCF/6-311+G(2d,2p) (and B3LYP/6-311+G(2d,2p) in brackets) optimized structures involved in the formation and cleavage of 1,2-dioxolane.

activation enthalpy is 33.6 kcal/mol (**TSA3**; Table 1, see the Supporting Information<sup>88</sup>). **MA4** can decompose via **TSA5** to yield formaldehyde and oxirane in an exothermic step setting free 44.1 kcal/mol. The reaction is probably initiated by anomeric delocalization of an O electron lone pair into the vicinal  $\sigma^*(CC)$  orbital thus weakening the CC bond. CC bond cleavage is also possible for **MA3** which decomposes via **TSA7**. The activation enthalpy of is 14.1 kcal/mol (DFT; CCSD(T), 14.1, Table 1) and leads to the biradical intermediate **MA5** (Figure 4) which decomposes quickly to oxirane as is described above. The total activation enthalpy for decomposition of **MA2** via **MA4** and **TSA5** to oxirane and formaldehyde is 39.3 and 44.3 kcal/mol via **MA3** and **TSA7**.

(b) Simultaneous cleavage of the O1O2 and C4C5 bonds in **MA2** requires an activation enthalpy of 41.1 kcal/mol (**TSA6**,

Figure 3) and yields biradical **MA5** + formaldehyde (see Figure 4). In view of the high barrier, this process is also less likely than the stepwise mechanism described above. **TSA6** presents a rather late TS as documented by calculated C••C and O••O distances of 2.05 and 2.86 Å, respectively (see Figure 3). Such a long OO distance is normally indicative of a stepwise rather than a concerted mechanism. However, the energy profile along the reaction path shows a shoulder rather than a minimum thus suggesting a highly asynchronous but still concerted process.

**IV.5. Formation of 1,3-Dioxolane.** Biradical **C** adds to **E** in a concerted fashion producing the five-membered ring of 1,3-dioxolane (**MC2**). The TS (**TSC1**) is preceded by a van der Waals complex (**MC1**). Both **MC1** and **TSC1** structures possess  $C_s$  symmetry and have strong biradical character, which is clearly reflected by the calculated geometries (compare the OCO



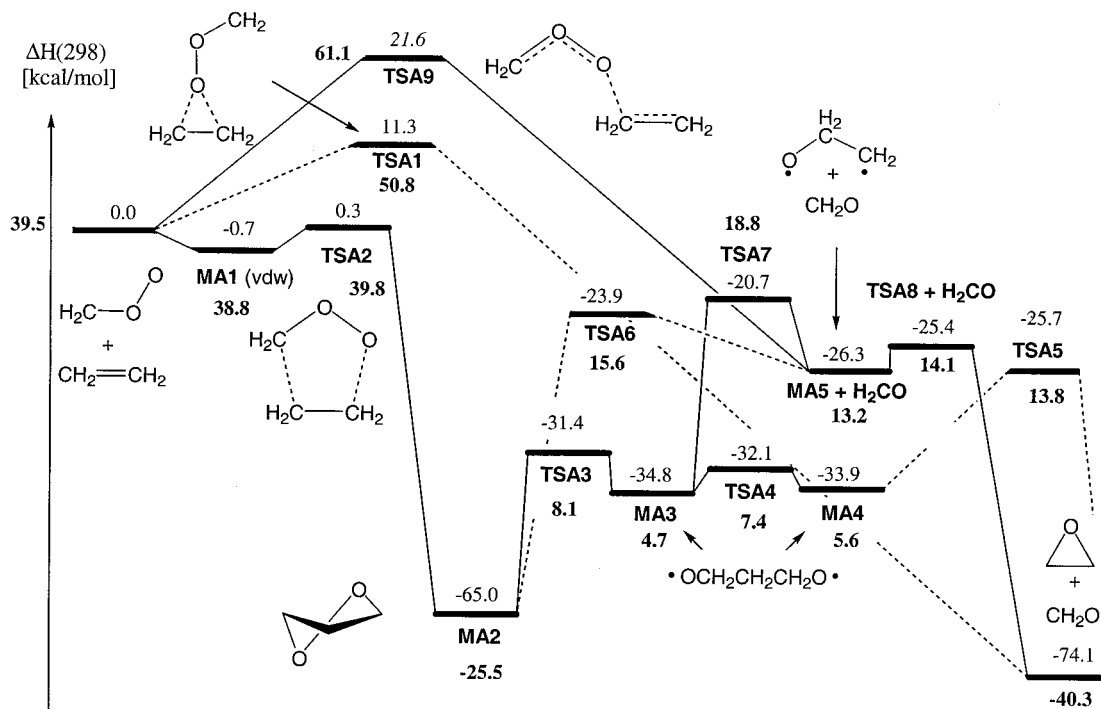


**Figure 4.** Schematic energy diagram of the reactions of carbonyl oxide (**A**) and ethylene (**E**). Heats of formation  $\Delta H_f^\circ(298)$  (bold print) and enthalpy differences relative to that of **A** (normal print) are given according to Table 1 (last column).

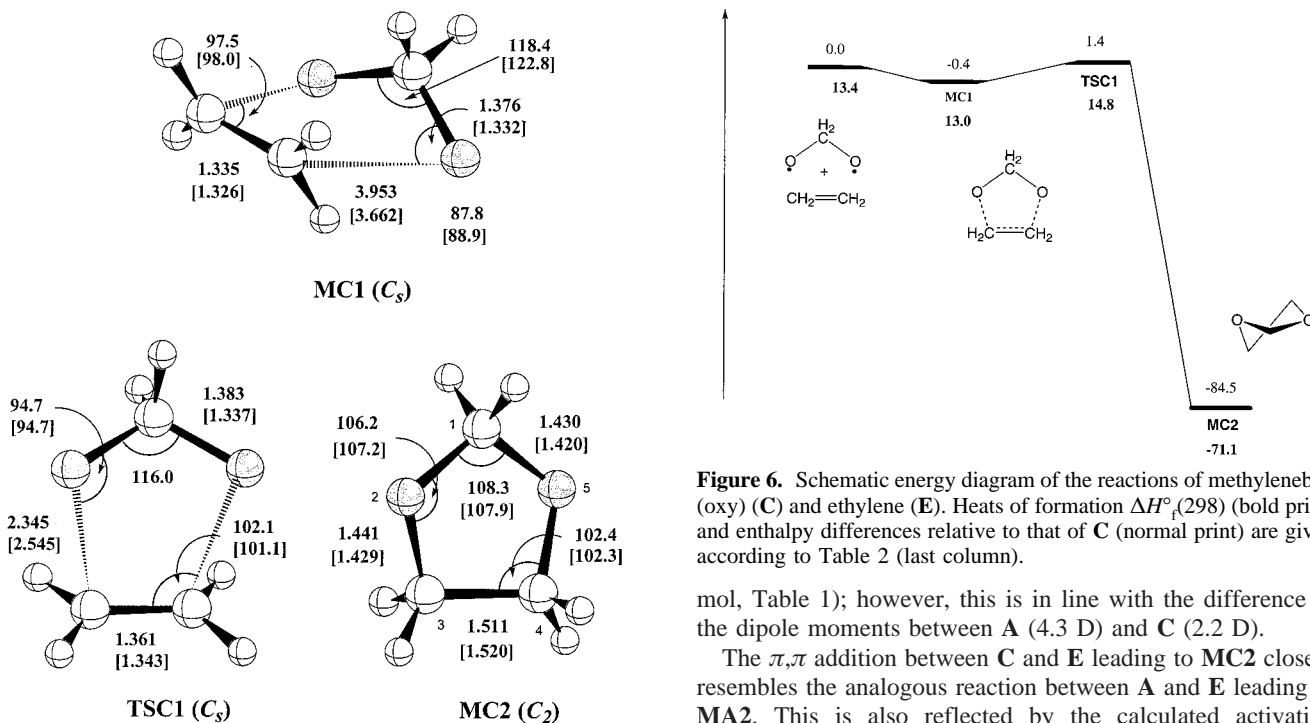


**Figure 5.** Selected geometrical parameters of the CASSCF/6-311+G-(2d,2p) (and B3LYP/6-311+G(2d,2p) in brackets) optimized structures involved in the formation of 1,3-dioxolane.

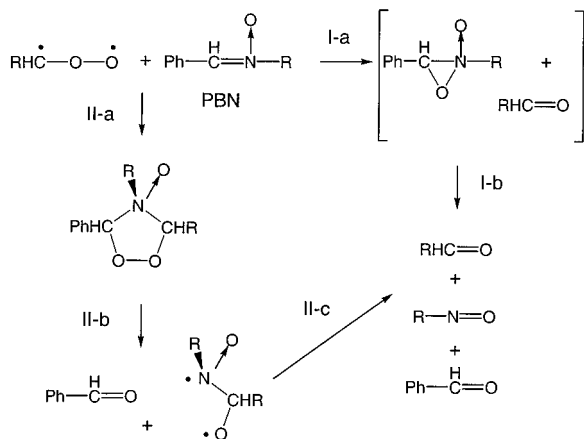
moiety of **MC1** and **TSC1** in Figure 5 with that of **C** in Figure 2) and the composition of the CASSCF wave function.<sup>90</sup> This is insofar interesting as **MC1** is to the best of our knowledge the first example of a van der Waals complex involving a biradical (for a van der Waals complex involving a radical, see ref 91). The complexation enthalpy is just 0.4 kcal/mol (after BSSE corrections;  $\Delta E = 1.4$  kcal/mol, Table 2) and by this smaller than for complex **MA1** (0.8 kcal/mol,  $\Delta E = 2.0$  kcal/

**Figure 6.** Schematic energy diagram of the reactions of methylenebis(oxy) (**C**) and ethylene (**E**). Heats of formation  $\Delta H_f^\circ(298)$  (bold print) and enthalpy differences relative to that of **C** (normal print) are given according to Table 2 (last column).

mol, Table 1); however, this is in line with the difference in the dipole moments between **A** (4.3 D) and **C** (2.2 D).

The  $\pi,\pi$  addition between **C** and **E** leading to **MC2** closely resembles the analogous reaction between **A** and **E** leading to **MA2**. This is also reflected by the calculated activation enthalpies (1.8 and 1.0 kcal/mol, Tables 1 and 2). A very low activation enthalpy was also computed for the reaction between **A** and formaldehyde leading to secondary ozonide,<sup>25,28,92</sup> which also starts from a van der Waals complex<sup>13</sup> and is lower than 1 kcal/mol. The formation of **MC2** is exothermic by 84.5 kcal/mol; that is, the five-membered ring is formed with so much excess energy that in the gas phase its decomposition is a direct consequence. If however energy dissipation is possible as in the solution phase, **MC2** will be rather stable ( $\Delta H_f^\circ(298) = -71.1$  kcal/mol). In the  $\pi,\pi$ -addition reaction, **MC2** is first formed in the  $C_s$ -symmetrical envelope form but this is located at the TS of ring pseudorotation.<sup>87</sup> The following of the reaction path at this point leads to the  $C_2$ -symmetrical twist or the

## SCHEME 4



inverted twist form, which is 0.8 kcal/mol more stable than the envelope form. **MC2** is less puckered (puckering amplitude  $q = 0.349 \text{ \AA}$ ; HF/6-31G(d), 0.321  $\text{ \AA}$ ;<sup>87</sup> expt, 0.38  $\text{ \AA}$ ;<sup>87</sup> B3LYP, 0.442  $\text{ \AA}$ ; for bond lengths, see Figure 5) than **MA2** where these differences result from the peroxide unit in **MA2** as was discussed by Cremer.<sup>87</sup>

### V. Chemical Relevance of Results

According to the ab initio investigation presented above, **A** will preferentially undergo a [4+2] cycloaddition reaction in the presence of **E** because (a) the formation of van der Waals complex **MA1** channels the molecule into the cycloaddition mode and (b) the activation enthalpy for epoxidation (11.3 kcal/mol) is 10 kcal/mol larger than that of the cycloaddition mode (1.0 kcal/mol). The major reaction product will be 1,2-dioxolane rather than oxirane.

This result sheds a new light on reports of alkene epoxidation by **AA**.<sup>1,30–33,95,96</sup> Apart from those cases, where bulky substituents may hinder the cycloaddition reaction, 1,2-dioxolanes rather than oxiranes will be formed primarily. Actually, there is no basis for the latter assumption because the electronic structure of **A** is closely related to that of other 1,3-dipolar molecules, and therefore, **AA** should react similar as ozone, diazomethanes, etc. which are known to easily undergo cycloaddition reactions both in the gas and solution phases.<sup>97</sup>

As one example for a cycloaddition of **AA** to alkene, which was erroneously interpreted as an epoxidation of alkene, we cite work by Pryor and Govindan entitled *Oxygen-Atom Transfer Reactions from a Carbonyl Oxide (Produced from 1,2,3-Trioxolane) to Electron-Deficient Unsaturated Compounds*.<sup>96</sup> In their article, the authors report that the reaction of  $\alpha$ -phenyl-*tert*-butyl nitron (PBN) and **AA** as a decomposition product of an intermediate primary ozonide leads to 2-methyl-2-nitrosopropane and explain this by the epoxidation step I–a followed by reaction I–b shown in Scheme 4. In view of the results of this work, epoxidation of PBN is unlikely. Instead, the results of Pryor and Govindan suggest the cycloaddition reaction II-a followed by steps II-b and II-c (Scheme 4). There are many other results in the ozonolysis literature, which deserve similar corrections.

There is actually experimental evidence for the formation of 1,2-dioxolanes. Kuczkowski<sup>35</sup> showed that the latter are formed when **A** can react either with methyl formate or methyl vinyl ether in the ozonolysis of the ether. Reiser and co-workers<sup>38</sup> investigated the reactivity and selectivity of formaldehyde, acetaldehyde, and propionaldehyde carbonyl oxides with several alkenes. Graziano and co-workers<sup>39</sup> studied the regio and

stereoselectivity of the cycloaddition of a carbonyl oxide to electron poor alkenes. Nojiima and co-workers<sup>36,37</sup> found that **AA**, generated by treating secondary ozonides with boron trifluoride-diethyl ether, add to alkenes in solution to form 1,2-dioxolanes. The Lewis acid  $\text{BF}_3$  acts as a catalyst for the cycloreversion reaction of the ozonide to yield ketone and **AA**. There is no experimental evidence whether 1,2-dioxolane formation proceeds in a concerted or in a stepwise manner involving, in the latter case, a complex between **AA** and the Lewis acid. Work is in progress to clarify this question.<sup>98</sup>

In view of the results obtained in this work and in order to investigate the reaction possibilities of **AA**, Sander's synthesis of dimesityl ketone O-oxide at  $-50 \text{ }^\circ\text{C}$ <sup>16</sup> provides a possibility of initiating a controlled reaction between substituted **A** and alkene in solution. Such a reaction would provide also the possibility of studying steric factors on the [4+2] cycloaddition reaction and clarifying whether epoxidation is competitive with cycloaddition in such a case.

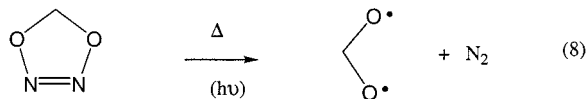
In the gas-phase ozonolysis, **A** is produced in a strongly exothermic process in a vibrationally excited state, which via rearrangement to **B** and **C** decomposes unimolecularly yielding  $\text{CO}_2$ ,  $\text{H}_2$ ,  $\text{CO}$ ,  $\text{H}_2\text{O}$ ,  $\text{H}$ ,  $\text{HCO}$ ,  $\text{OH}$ ,  $\text{O}$ , and  $\text{HCOOH}$  (see reaction 1).<sup>19–28</sup> However, a considerable fraction of **A** can be collisionally stabilized and may undergo bimolecular reactions.<sup>8–10,25</sup> It is known that stabilized alkyl-**AA** can react in the troposphere (or conditions relevant to smog chamber experiments) with aldehydes,  $\text{SO}_2$ ,  $\text{CO}$ ,  $\text{H}_2\text{O}$ , and  $\text{NO}_x$ , where the reaction with water vapor will be the major loss process under tropospheric conditions.<sup>8–10</sup> Reactions of **AA** with alkenes have not been reported for the gas phase, which simply reflects the fact that the concentration of alkene is generally too low under the experimental conditions. The situation may be different in several tropospheric conditions. The monoterpenes emitted by conifers and isoprene emitted by deciduous trees and other vegetation, the trace gas emissions from biomass fires, and the hydrocarbon emissions from vehicular exhaust and gasoline evaporation sources<sup>99</sup> can lead locally to larger alkene concentrations. However, no investigation has been reported considering this aspect.

If a cycloaddition reaction with alkene is not possible, **A** will undergo an epoxidation reaction where it should react faster than **B** according to the calculated activation enthalpies of 11.3 and 13.7 kcal/mol (Table 1) and in line with general expectations. However, the difference in reaction rates should be smaller than is generally assumed.

So far, **C** or one of its derivatives could not be detected. Evidence for the existence of **C** is only of indirect nature<sup>1–7</sup> or is based on quantum chemical investigations.<sup>27,28</sup> Hence, **C** is expected as an intermediate in decomposition/rearrangement reactions of **B** where theory predicts low kinetic and thermodynamic stability for the biradical.<sup>27,28</sup> There are three reactions of **C** with almost equal activation enthalpies, namely, H migration and rearrangement to formic acid (1.8 kcal/mol), decomposition to  $\text{CO}_2$  and  $\text{H}_2$  (2.4 kcal/mol), and the bimolecular addition to **E** (1.8 kcal/mol).<sup>27</sup> In the gas phase, unimolecular reactions of **C** will be preferred and explain the decomposition to  $\text{CO}_2$ ,  $\text{H}_2$ ,  $\text{H}_2\text{O}$ , and  $\text{CO}$  as has been discussed in detail by Cremer and co-workers.<sup>27</sup> In solution phase, ester formation from dioxiranes was observed, which will proceed via substituted **C** and alkyl group or aryl group migration. Actually, there is little chance of capturing **C** by adding an excess of alkene because **C** has to be generated via **B**, and **B**

will epoxidize alkene rather than open to **C** because of the relative magnitude of the corresponding barriers (13.7 and 18.0 kcal/mol<sup>27</sup>).

We conclude that **C** has to be generated in a different way under matrix isolation conditions to investigate its reactive behavior. The thermal (photochemical) decomposition of 3,5-dioxo-1,2-diazole (reaction 8) below 10 K in the presence of a suitable alkene monitored by IR spectroscopy possible is.



## VI. Conclusions

(1) According to the ab initio calculations carried out in this work, carbonyl oxides undergo preferentially cycloaddition reactions with alkenes (activation enthalpy, 1.0 kcal/mol) yielding 1,2-dioxolanes, whereas dioxiranes preferentially undergo epoxidation reactions (13.7 kcal/mol), which are faster than ring opening to methylenebis(oxy) biradicals (18.0 kcal/mol<sup>27</sup>).

(2) The results of the present investigation give theoretical mechanistic support to the observation of 1,2-dioxolanes in experiments reported in the literature.<sup>35–39</sup> Experimental evidence for the epoxidation of alkenes by carbonyl oxides results from the fact that 1,2-dioxolanes formed in an alkene–carbonyl oxide cycloaddition reaction decompose to oxirane and aldehyde because of the high excess energy generated when forming the dioxolane.

(3) Direct epoxidation of alkene by carbonyl oxide can only be expected in the situation of an alkene with bulky substituents at the double bond (steric hindrance of the cycloaddition reaction). In this case, epoxidation by carbonyl oxide will be somewhat faster than epoxidation by dioxirane in view of the calculated activation enthalpies of 11.3 and 13.7 kcal/mol. In both cases, epoxidation should be stereo- and regioselective in view of the similar MO interaction patterns derived for the two reactions (Scheme 2). Differences will only arise from the fact that carbonyl oxides should be more nucleophilic than dioxiranes.

(4) Experiments are suggested (reactions with dimesityl ketone O-oxide) to experimentally verify the influence of steric factors on the cycloaddition reaction between carbonyl oxides and alkenes and to clarify whether epoxidation may be competitive in such a case.

(5) Dioxymethylenes should preferentially add to alkenes forming 1,3-dioxolanes. However, there will be no chance of observing this reaction if the biradicals are formed by rearrangement of carbonyl oxides or dioxiranes. An experiment is suggested to isolate dioxymethylenes and study the cycloaddition reaction.

(6) We report for the first time theoretical evidence for the possibility of a van der Waals complex between a biradical and a closed shell molecule, which also may be studied in a suitable matrix isolation experiment.

(7) The reactions of **A**, **B**, and **C** with **E** (alkenes) can be understood as concerted  $\sigma-\pi$  or concerted  $\pi-\pi$  reactions on the basis of FMO theory and the Woodward–Hoffmann rules. We emphasize that 1,3-dipolar molecules and 1,3-biradicals have a similar reactive behavior, which originates in their common biradical character.

(8) We have derived reliable heats of formation for all molecules and TSs considered in this work. Comparison of CASPT2, CCSD(T), and DFT/B3LYP results reveals that the

latter are surprisingly accurate also for systems with high biradical character. However, deficiencies of DFT in calculating TSs becomes also obvious. A particular problem has been the sensitivity of CASPT2 with regard to relative small changes in the decomposition of the active space. UHF–CCSD(T) performs well in the case of biradicals in agreement with the expectations given in ref 62.

The present investigation establishes a basis for studying larger substituted systems directly relevant for ongoing experiments.

**Acknowledgment.** This research was supported by the Direcció General de Investigació Científica y Tècnica (DGI-CYT, Grants PB98-1240-C02-01 and PB98-1240-C02-02) at Barcelona and by the Swedish Natural Science Research Council (NFR) at Göteborg, R.C. thanks the CIRIT (de Catalunya, Spain) for financial support. The calculations described in this work were performed on the supercomputers of the CESCA (Barcelona), on the SGI Power Challenge at CSIC, and at the supercomputers of the NSC (Linköping).

**Supporting Information Available:** The full set of results (Cartesian coordinates of all stationary points and all CASSCF, CCSD(T), CASPT2, and B3LYP absolute energies of all structures). This material is available free of charge via the Internet at <http://pubs.acs.org>.

## References and Notes

- Bailey, P. S. In *Ozonation in Organic Chemistry*; Academic Press: New York, 1968; Vols. I and II.
- Bunnelle, W. H. *Chem. Rev.* **1991**, *91*, 335.
- Baumstark, A. L. *Advances in Oxygenated Processes*; JAI Press, Inc., Greenwich, CN, 1990; Vol. 2.
- Kuczowski, R. L. *Ozone and Carbonyl Oxides*. In *1,3-Dipolar Cycloaddition Chemistry*; Padwa, A., Ed.; Wiley: London, 1984; Vol. 2, Chapter 11, p 197.
- Sander, W. *Angew. Chem.* **1990**, *102*, 362; *Angew. Chem., Int. Ed. Engl.* **1990**, *29*, 344.
- (a) Murray, R. W. *Chem. Rev.* **1989**, *89*, 1187. (b) Murray, R. W. In *Molecular Structure and Energetics. Unconventional Chemical Bonding*; Liebman, J. F., Greenberg, A., Eds.; VCH Publishers: New York, 1988; Vol. 6, p 311.
- Kafafi, S. A.; Martinez, R. I.; Herron, J. T. In *Molecular Structure and Energetics. Unconventional Chemical Bonding*; Liebman, J. F., Greenberg, A., Eds.; VCH Publishers: New York, 1988; Vol. 6.
- (a) Atkinson, R. *Atmos. Environ.* **2000**, *34*, 2063. (b) Atkinson, R. *Atmos. Environ.* **1990**, *24A*, 1.
- Horie, O.; Mortgat, G. K. *Acc. Chem. Res.* **1998**, *31*, 387.
- Carter, W. P. L. *Atmos. Environ.* **1990**, *24A*, 481.
- (a) Criegee, R. *Angew. Chem., Internat. Edit.* **1975**, *14*, 745. (b) Criegee, R.; Wenner, G. *Liebigs Ann. Chem.* **1949**, *564*, 9.
- (a) Suenram, R. D.; Lovas, F. J. *J. Am. Chem. Soc.* **1978**, *100*, 5117. (b) Lovas, F. J.; Suenram, R. D. *Chem. Phys. Lett.* **1977**, *51*, 453.
- Cremer, D.; Kraka, E.; McKee, M. L.; Radhakrishnan, T. P. *Chem. Phys. Lett.* **1991**, *187*, 491.
- (a) Scaiano, J. C.; McGimpsey, W. G.; Casal, H. L. *J. Org. Chem.* **1989**, *54*, 1612. (b) Casal, H. L.; Tanner, M.; Werstki, N. H.; Scaiano, J. C. *J. Am. Chem. Soc.* **1985**, *107*, 4616.
- Block, K.; Kapert, W.; Kirschfeld, A.; Muthusamy, S.; Schroeder, K.; Sander, W.; Kraka, E.; Sosa, C.; Cremer, D. In *Peroxide Chemistry—Mechanistic and Preparative Aspects of Oxygen Transfer*; Adam, W., Ed.; Wiley-VCH: Weinheim, Germany, 2000; p 139.
- (a) Kirschfeld, A.; Muthusamy, S.; Sander, W. *Angew. Chem.* **1994**, *106*, 2261; *Angew. Chem., Int. Ed. Engl.* **1994**, *33*, 2212. (b) Sander, W.; Kirschfeld, A.; Kappert, W.; Muthusamy, S.; Kiselevsky, M. *J. Am. Chem. Soc.* **1996**, *118*, 6508.
- (a) Kraka, E.; Sosa, C. P.; Cremer, D. *Chem. Phys. Lett.* **1996**, *260*, 43. (b) Sander, W.; Block, K.; Kappert, W.; Kirschfeld, A.; Muthusamy, S.; Schroeder, K.; Sosa, C. P.; Kraka, E.; Cremer, D. *J. Am. Chem. Soc.* **2001**, *123*, 2618. (c) Cremer, D.; Kraka, E.; Sosa, C. *Chem. Phys. Lett.* **2001**, *337*, 199.
- Sander, W.; Schroeder, K.; Muthusamy, S.; Kirschfeld, A.; Kappert, W.; Boese, R.; Kraka, E.; Sosa, C.; Cremer, D. *J. Am. Chem. Soc.* **1997**, *119*, 7265.
- Herron, J. T.; Huie, E. *J. Am. Chem. Soc.* **1977**, *99*, 5430.



- (20) Gäb, S.; Hellpointner, E.; Turner, W. V.; Korte, F. *Nature* **1985**, *316*, 535.
- (21) Niki, H.; Maker, P. D.; Savage, C. M.; Breitenbach, L. P.; Hurley, M. D. *J. Phys. Chem.* **1987**, *91*, 941.
- (22) (a) Martinez, R. I.; Herron, J. T. *J. Phys. Chem.* **1987**, *91*, 946. (b) Martinez, R. I.; Herron, J. T. *J. Phys. Chem.* **1988**, *92*, 4644.
- (23) Cremer, D.; Gauss, J.; Kraka, E.; Stanton, J. F.; Bartlett, R. J. *Chem. Phys. Lett.* **1993**, *209*, 547.
- (24) Anglada, J. M.; Bofill, J. M.; Olivella, S.; Solé, A. *J. Am. Chem. Soc.* **1996**, *118*, 4636.
- (25) Olzmann, M.; Kraka, E.; Cremer, D.; Gutbrod, R.; Andersson, S. *J. Phys. Chem.* **1997**, *101*, 9421.
- (26) Anglada, J. M.; Bofill, J. M.; Olivella, S.; Solé, A. *J. Phys. Chem. A* **1998**, *10*, 3398.
- (27) Cremer, D.; Kraka, E.; Szalay, P. G. *Chem. Phys. Lett.* **1998**, *292*, 97.
- (28) (a) Anglada, J. M.; Crehuet, R.; Bofill, J. M. *Chem. Eur. J.* **1999**, *5*, 1809. (b) Anglada, J. M.; Besalú, E.; Bofill, J. M.; Crehuet, R. *J. Comput. Chem.* **1999**, *20*, 1130. (c) Anglada, J. M.; Bofill, J. M.; Olivella, S.; Solé, A. *J. Phys. Chem. A* **1998**, *102*, 3398.
- (29) Cremer, D.; Bock, C. W. *J. Am. Chem. Soc.* **1986**, *108*, 3375.
- (30) Bach, R. D.; Owensby, A. L.; Andrés, J. L.; Schlegel, H. B. *J. Am. Chem. Soc.* **1991**, *113*, 7031.
- (31) Bach, R. D.; Andrés, J. L.; Owensby, A. L.; Schlegel, H. B.; McDouall, J. J. W. *J. Am. Chem. Soc.* **1992**, *114*, 7207.
- (32) Bach, R. D.; Glukhovtsev, M. N.; Gonzalez, C.; Marquez, M.; Estévez, C. M.; Baboul, A. G.; Schlegel, H. B. *J. Phys. Chem. A* **1997**, *101*, 6092.
- (33) Baboul, A. G.; Schlegel, H. B.; Glukhovtsev, M. N.; Bach, R. D. *J. Comput. Chem.* **1998**, *19*, 1353.
- (34) Cremer, D. In *The Chemistry of Functional Groups, Peroxides*; Patai, S., Ed.; Wiley: New York, 1983; p 1.
- (35) (a) Keul, H.; Kuczowski, R. L. *J. Am. Chem. Soc.* **1984**, *105*, 5370. (b) Keul, H.; Kuczowski, R. L. *J. Org. Chem.* **1985**, *50*, 3371. (c) Keul, H.; Choi, H. S.; Kuczowski, R. L. *J. Org. Chem.* **1985**, *50*, 3365. (d) Wojciechowski, B. J.; Pearson, W. H.; Kuczowski, R. L. *J. Org. Chem.* **1989**, *54*, 115.
- (36) Miura, M.; Yoshida, M.; Nojima, M.; Kusabayashi, S. *J. Chem. Soc., Chem. Commun. Com.* **1982**, *1493*, 397.
- (37) Yoshida, M.; Miura, M.; Nojima, M.; Kusabayashi, S. *J. Am. Chem. Soc.* **1983**, *105*, 6279.
- (38) Reiser, R.; Süling, C.; Schröder, G.; *Chem. Ber.* **1992**, *125*, 2493
- (39) Graziano, M. L.; Iesce, M. R.; Cermola, F.; Giordano, F.; Scarpati, R. *J. Chem. Soc. Chem. Commun.* **1989**, 1608.
- (40) Wadt, W. R.; Goddard, W. A., III. *J. Am. Chem. Soc.* **1975**, *97*, 3004.
- (41) Ring **B** ( $C_{2v}$  symmetry) is mainly characterized by the closed shell ( $..6a_1^2 3b_2^2 2b_1^2 1a_2^2$ ) electron configuration, whereas the acyclic isomers **A** ( $C_s$  symmetry) and **C** ( $C_{2v}$  symmetry) are characterized by electron configurations  $0.94 [..10a_1^2 1a''^2 2a''^2] - 0.22 [..10a_1^2 1a''^2 3a''^2]$  and  $0.78 [..6a_1^2 4b_2^2 1b_1^2 1a_2^2] - 0.56 [..6a_1^2 4b_2^2 1b_1^2 2b_1^2]$ , respectively, according to the calculations carried out in this work (see section III). The magnitude of the squared coefficients of the two leading configurations can be considered to reflect the biradical character of these species. The  $b_1$ ,  $a_2$ , or  $a''$  orbitals are  $\pi$ -type orbitals (Schemes 2 and 3), and the projection of the configurations of **C** into  $C_s$  symmetry leads to comparable electronic descriptions for **C** and **A**, in particular if the pseudo- $\pi$ (CH<sub>2</sub>) orbital of **C** is included into the description. Also, the MOs from **A** and **C** have similar topologies although they are more asymmetric in the case of carbonyl oxide.
- (42) (a) Dewar, M. J. S. *Nature* **1945**, *156*, 748. (b) Dewar, M. J. S.; Ford, G. P. *J. Am. Chem. Soc.* **1979**, *101*, 183.
- (43) (a) Cremer D.; Kraka, E. *J. Am. Chem. Soc.* **1985**, *107*, 3800. (b) Kraka E.; Cremer, D. In *Theoretical Models of Chemical Bonding. The Concept of the Chemical Bond*; Maksic, Z. B., Ed.; SpringerVerlag: Heidelberg, Germany, 1990; Vol. 2, p 453.
- (44) Yamaguchi, K. *J. Mol. Struct.* **1983**, *103*, 101.
- (45) Banichevich, A.; Peyerimhoff, S. D. *Chem. Phys.* **1993**, *174*, 93.
- (46) Roos, B. O. *Adv. Chem. Phys.* **1987**, *69*, 399.
- (47) Baker, J. J. *J. Comput. Chem.* **1986**, *7*, 385.
- (48) Baker, J. J. *J. Comput. Chem.* **1987**, *8*, 563.
- (49) (a) Bofill, J. M. *J. Comput. Chem.* **1994**, *15*, 1. (b) Bofill, J. M.; Comajuan, M. *J. Comput. Chem.* **1995**, *16*, 1326.
- (50) Anglada, J. M.; Bofill, J. M. *Chem. Phys. Lett.* **1995**, *243*, 151.
- (51) Buenker, R. J.; Peyerimhoff, S. D. *Theor. Chim. Acta* **1975**, *39*, 217.
- (52) Buenker, R. J.; Peyerimhoff, S. D. In *New Horizons of Quantum Chemistry*; Lowdin, P. O., Pullman, B., Eds.; D. Reidel: Dordrecht, The Netherlands, 1983; Vol. 35, p 183.
- (53) Buenker, R. J.; Phillips, R. A. *J. Mol. Struct. (THEOCHEM)* **1985**, *123*, 291.
- (54) Hariharan, P. C.; Pople, J. A. *Theor. Chim. Acta* **1973**, *28*, 213.
- (55) (a) Fukui, K. *J. Phys. Chem.* **1970**, *74*, 4161. (b) Fukui, K. *Acc. Chem. Res.* **1981**, *14*, 363.
- (56) Curtiss, L. A.; Raghavachari, K.; Trucks, G. W.; Pople, J. A. *J. Chem. Phys.* **1991**, *94*, 7221.
- (57) Krishnan, R.; Binkley, J. S.; Seeger, R.; Pople, J. A. *J. Chem. Phys.* **1980**, *72*, 650.
- (58) Anderson, K.; Malmqvist, P. A.; Roos, B. O. *J. Chem. Phys.* **1992**, *96*, 1218.
- (59) Cizek, J. *Adv. Chem. Phys.* **1969**, *14*, 35.
- (60) Raghavachari, K.; Trucks, G. W.; Pople, J. A.; Head-Gordon, M. *Chem. Phys. Lett.* **1989**, *157*, 479.
- (61) (a) Lee, T. J.; Taylor, P. R. *Int. J. Quantum Chem. Symp.* **1989**, *23*, 199. (b) Jayatilaka, D.; Lee, T. J. *J. Chem. Phys.* **1993**, *12*, 9734.
- (62) He, Y.; Cremer, D. *Chem. Phys. Lett.* **2000**, *324*, 389.
- (63) Boys, S. F.; Bernardi, F. *Mol. Phys.* **1970**, *19*, 553.
- (64) Becke, A. D. *J. Chem. Phys.* **1993**, *98*, 5648.
- (65) Scott, A. P.; Radom, L. *J. Phys. Chem.* **1996**, *100*, 16502.
- (66) He, Y.; Gräfenstein, J.; Kraka, E.; Cremer, D. *Mol. Phys.* **2000**, *98*, 1639.
- (67) (a) Gräfenstein, J.; Kraka, E.; Cremer, D. *Chem. Phys. Lett.* **1998**, *288*, 593.
- (68) Gräfenstein, J.; Hjerpe, A.; Kraka, E.; Cremer, D. *J. Phys. Chem. A* **2000**, *104*, 1748.
- (69) (a) Gräfenstein J.; Cremer, D. *Chem. Phys. Lett.* **2000**, *316*, 569. (b) Gräfenstein, J.; Cremer, D. *Phys. Chem. Chem. Phys.* **2000**, *2*, 2091. (c) Gräfenstein, J.; Kraka, E.; Filatov, M.; Cremer, D. *J. Phys. Chem.* Submitted for publication.
- (70) (a) Cox, J. D.; Pilcher, G. *Thermochemistry of Organic and Organometallic Compounds*; Academic Press: London, 1970. (b) NIST Standard Reference Database 25, version 2.02; National Institute of Standards and Technology: Gaithersburg, MD, 1994. (c) Pedley, J. B.; Naylor, R. D.; Kirby, S. P. *Thermochemical Data of Organic Compounds*; Chapman and Hall: New York, 1986. (d) Chase, M. W., Jr. *J. Phys. Chem. Ref. Data*, **1998**, *Monograf* 9, 1. (e) <http://webbook.nist.gov>.
- (71) Benson, S. W. *Thermochemical Kinetics*; John Wiley: New York, 1968.
- (72) Schmidt, M. W.; Baldrige, K. K.; Boatz, J. A.; Jensen, J. H.; Koseki, S.; Gordon, M. S.; Nguyen, K. A.; Windus, T. L.; Elbert, S. T. *QCPE Bull.* **1990**, *10*, 52.
- (73) Frisch, M. J.; Trucks, G. W.; Schlegel, H. B.; Gill, P. M. W.; Johnson, B. G.; Robb, M. A.; Cheeseman, J. R.; Keith, T.; Petersson, G. A.; Montgomery, J. A.; Raghavachari, K.; Al-Laham, M. A.; Zakrzewski, V. G.; Ortiz, J. V.; Foresman, J. B.; Cioslowski, J.; Stefanov, B. B.; Nanayakkara, A.; Challacombe, M.; Peng, C. Y.; Ayala, P. Y.; Chen, W.; Wong, M. W.; Andres, J. L.; Replogle, E. S.; Gomperts, R.; Martin, R. L.; Fox, D. J.; Binkley, J. S.; Defrees, D. J.; Baker, J.; Stewart, J. P.; Head-Gordon, M.; Gonzalez, C.; Pople, J. A. *Gaussian 94*; Gaussian, Inc: Pittsburgh, PA, 1995.
- (74) Anderson, K.; Fülischer, M. P.; Lindh, R.; Malmqvist, P. A.; Olsen, J.; Roos, B. O.; Sadlej, A. J.; Widmark, P. O. *Molcas 4.1*; University of Lund and IBM: Lund, Sweden, 1991.
- (75) Wierlacher, S.; Sander, W.; Marquardt, C.; Kraka, E.; Cremer, D. *Chem. Phys. Lett.* **1994**, *222*, 319.
- (76) (a) Kim, S. J.; Schaefer, H. F.; Kraka, E.; Cremer, D. *Mol. Phys.* **1996**, *88*, 93. (b) Kraka, E.; Konkoli, Z.; Cremer, D.; Fowler, J.; Schaefer, H. F. *J. Am. Chem. Soc.* **1996**, *118*, 10595.
- (77) (a) Gutbrod, R.; Schindler, R. N.; Kraka E.; Cremer, D. *Chem. Phys. Lett.* **1996**, *252*, 221. (b) Gutbrod, R.; Kraka, E.; Schindler, R. N.; Cremer, D. *J. Am. Chem. Soc.* **1997**, *119*, 7330.
- (78) Stanton, J. F.; Lopreore, C.; Gauss, J. *J. Chem. Phys.* **1998**, *108*, 7190.
- (79) The CASPT2 calculations reported in Tables 1 and 2 for **A**, **B**, and **C** are based on a CASSCF(8,8) reference function. To check the reliability of these results, we have performed additional single-point CASPT2 calculations on **B** and **C**, which are based on different CASSCF reference functions. The computed CASPT2 energy differences  $E(\mathbf{B}) - E(\mathbf{C})$  are 10.2, 6.9, 5.1, and 6.2 kcal/mol when using a CASSCF reference functions with a (6,4), (8,8), (12,11), and (18,14) active space. The last three values are in the range of the energy differences computed with multireference methods (MRD-CI<sup>26</sup> or MR-CC<sup>27</sup>). These energy differences are about 5 kcal/mol lower than the corresponding UHF-CCSD(T) value. However, the T1 diagnostic for **C** is 0.025 thus indicating the need to use a multireference method for a correct description of this biradical.
- (80) Anglada, J. M.; Bofill, J. M.; Crehuet, R. Unpublished results.
- (81) Gillies, C. W.; Gillies, J. Z.; Suenram, R. D.; Lovas, F. J.; Kraka, E.; Cremer, D. *J. Am. Chem. Soc.* **1991**, *113*, 2412.
- (82) McKee, M. L.; Rohlffing, C. M. *J. Am. Chem. Soc.* **1989**, *111*, 2497.
- (83) Cremer, D. *J. Chem. Phys.* **1978**, *70*, 1898.
- (84) (a) Cremer, D. *J. Am. Chem. Soc.* **1981**, *103*, 3619–26. (b) Cremer, D. *J. Am. Chem. Soc.* **1981**, *103*, 3627.
- (85) (a) Zozom, J.; Gillies, C. W.; Suenram, R. D.; Lovas, F. J. *J. Chem. Phys. Lett.* **1987**, *139*, 64. (b) Gillies, J. Z.; Gillies, C. W.; Suenram, R. D.; Lovas, F. J. *J. Am. Chem. Soc.* **1988**, *110*, 7991.
- (86) Kan, C. S.; Calvert, J. G.; Shaw, J. H. *J. Phys. Chem.* **1981**, *85*, 2359.



- (87) Cremer, D. *Isr. J. Chem.* **1983**, 23, 72.
- (88) See, e.g., Baker, J.; Muir, M.; Andzelm, J.; Schreiner, A. In *Chemical Applications of Density Functional Theory*; Laird, B. B., Ross R. B., Ziegler, T., Eds.; ACS Symposium Series 629, American Chemical Society: Washington, DC, 1996; p 342.
- (89) Anglada, J. M.; Cremer, D.; Bofill, J. M.; Crehuet, R. To be published.
- (90) The electronic configuration describing both **MC1** and **TSC1** is given by  $c_1 12a^28a'^2 + c_2 13a^27a'^2$ , where the coefficients  $c_1$  and  $c_2$  are +0.75 and -0.57 for **MC1** and +0.82 and -0.47 for **TSC1**, respectively. Thus, the biradical character of the reacting **C** (+0.78 and -0.56, see chapter II) is maintained in both the van der Waals complex and the TS.
- (91) Wrobel, R.; Sander, W.; Kraka, E.; Cremer, D. *J. Phys. Chem. A* **1999**, 103, 3693.
- (92) Aplincourt, P.; Ruiz-López, M. F. *J. Phys. Chem. A* **2000**, 104, 380.
- (93) Lide, D. R., Ed.; *The Handbook of Chemistry and Physics*, 72nd ed.; CRC Press: Boca Raton, FL, 1991.
- (94) See, e.g., Woodward, R. B.; Hoffmann, R. *Angew. Chem., Int. Ed. Engl.* **1969**, 8, 781.
- (95) (a) Adam, W.; Sanabia, J. *J. Am. Chem. Soc.* **1977**, 99, 2735. (b) Adam, W.; Duran, N. *J. Am. Chem. Soc.* **1977**, 99, 2729.
- (96) Pryor, W. A.; Govindan, C. K. *J. Am. Chem. Soc.* **1981**, 103, 7681.
- (97) Padwa, A., Ed.; *1,3-Dipolar Cycloaddition Chemistry*; Wiley: London, 1984; Vols. 1 and 2.
- (98) Cremer, D.; Anglada, J. M.; Schmidt, T. To be published.
- (99) (a) Finlayson-Pitts, B. J.; Pitts, J. N. *Atmospheric Chemistry, Fundamentals and Experimental Techniques*; Wiley-Interscience: New York, 1986. (b) Yokelson, R. J.; Goode, J. G.; Ward, D. E.; Susott, R. A.; Babbitt, R. E.; *J. Geophys. Res.* **1999**, 104, 30109. (c) Goode, J. G.; Yokelson, R. J. *Geophys. Res.* **1999**, 104, 21237. (d) Sharma, U. K.; Kajii, Y.; Akimoto, H. *Atmos. Environ.* **2000**, 34, 3297, (e) Wayne, R. P. *Chemistry of Atmospheres*, 3rd ed.; Oxford University Press: Oxford, U.K., 2000.